VOL. 6, NO. 5, MAY 2011 ISSN 1819-6608
ARPN Journal of Engineering and Applied Sciences

www.arpnjournals.com

BEHAVIOR OF ULTRA HIGH PERFORMANCE CONCRETE STRUCTURES

Adel A. Al-Azzawi, Ahmed Sultan Ali and Husam K. Risan
Department of Civil Engineering, Nahrain University, Baghdad, Iraq
E-Mail: dr_adel_azzawi@yahoo.com

ABSTRACT

A study has been made through this investigation to understand the behavior of UHPC members with steel fibers by using two approaches: experimental investigation of concrete mixes and simulation of the problem studied by other researchers using finite elements. Experimental investigation is carried out to obtain the mechanical properties for two types of UHPC mixes, namely, the type of pozzolanic admixture (Silica Fume and High Reactivity Metakaolin) in addition to use three different values of steel fibers volume fraction (1%, 1.5% and 2%). The finite element method through the ANSYS computer program is used. The eight node brick element is used to model the UHPC beams with embedded steel fibers. The stress-strain curve in compression for the UHPC with steel fibers is simulated by a nonlinear elasto-plastic model which is terminated at the onset the crushing. In tension, a smeared crack model with fix orthogonal cracks has been used. The experimental data obtained from other researchers is compared with the finite element solution and good agreement between the results is obtained. Parametric studies are carried out to investigate the effects of type of pozzolanic admixture, volume fraction of steel fibers and other solution parameters. Higher values of compressive strength have been achieved using UHPC mixes with Silica Fume in comparison with UHPC mix with High Reactivity Metakaolin.

Keywords: concrete structures, ultra high performance, behavior, metakaolin, silica fume, steel fibers, ANSYS.

1. INTRODUCTION

The term Ultra High Performance Concrete (UHPC) has been used to describe a fiber-reinforced, superplasticized, silica fume-cement mixture with very low water-cement ratio (*w/c*) characterized by the presence of very fine quartz sand (0.15-0.40 mm) instead of ordinary aggregate [1] The absence of coarse aggregate was considered by the inventors to be a key-aspect for the microstructure and the performance of the UHPC in order to reduce heterogeneity between the cement matrix and the aggregate. However, due to the use of very fine sand instead of ordinary aggregate, the cement density of UHPC is as high as (900-1000 kg/m^3)[2]. One of the primary benefits of this class of concrete is that it can exhibit significant tensile strength and toughness. Much of such properties enhancement is imparted to the concrete by the addition of short, discontinuous fibers during the mixing procedure [3]. In fact there are limited studies on Ultra High Performance or Reactive Powder Concrete, and this section presents a review of such studies.

Collepardi *et al*. (1996) [2] studied the influence of the super-plasticizer type on the compressive strength of reactive powder concrete RPC. Two types of Portland cement were used having different C_3A content. Also three silica fume brands were used which were different with respect to both color (white, gray and dark) and particle size. Three different super-plasticizers were also used (a- Acrylic Polymer AP, b- Sulfonated Melamine SMF, c- Sulfonated Naphthalene SNF), and the results regarding w/cementitious ratio and compressive strength were examined. It was found that the Acrylic Polymer (AP) admixture performed better than the naphthalene (SNF) or melamine (SMF) based super-plasticizers in regard to lower water cementitious ratio and higher compressive strength at ages exceeding 3 days.

Roux *et al*. (1996) [4] investigated the durability of RPC. Two RPC mixes were tested; the sole difference between the specimens produced was in the casting technique. The first one was table-vibrated in the laboratory (RPC200), whereas the second was pressurized before and during setting (RPC200c) with the pressure of 60MPa. The extremely high resistance of RPC200 and RPC200c concrete to the penetration of aggressive agents corresponds to excellent durability characteristics, thereby yielding a significant increase in the life expectancy of structures built with Reactive Powder Concretes.

Qian and Li (2001) [5] reported the results of a study of stress - strain relationships (tension and compression) and flexural strength measurements for concrete incorporating 0%, 5%, 10%, and 15% metakaolin. The test results show that the tensile strength and peak strain increase with increasing metakaolin content whereas the tensile elastic modulus shows only small changes. The descending area of over-peak stress is improved when 5% and 10% of cement is replaced by metakaolin. Also, the modulus of rupture and compressive strength increase with increasing metakaolin content. The compressive elasticity modulus of concrete shows a small increase with increasing metakaolin replacement.

Lubbers (2003) [1] stated that UHPC could have a compressive strength 2 to 3 times greater than High Performance Concrete (HPC) and a flexural strength 2 to 6 times greater, and such mechanical properties of UHPC make it ideal for prestressing applications. It was also stated that before UHPC could be used in a prestressing application, bond performance between the UHPC and the prestressing strands had to be seriously investigated.

Stähli and Mier (2004) [6] studied the ratio between tensile and an ultra-high compressive strength of cementitious materials such as RPC. It was concluded that the compressive strength could be produced for RPC but not necessarily lead to the improvement of the compressive-tensile strength ratio (c/t-ratio). Attempt was made to reduce the c/t ratio from 10:1 (which is typical for an ordinary fiber reinforced concrete) to an ideal ratio of 1:1.

Schneider *et al*. (2004) [7] carried out a series of tests on stub composite columns under concentric loading. The filling consists of concrete of a wide strength range. Normal Strength concrete (NS 36MPa), High Strength concrete (HS 96MPa) and Ultra High Performance Concrete (UHPC 160MPa) were used. The load was applied exclusively on the concrete sections so that the load bearing behavior of the confined concrete core could be tested. Comparatively the load carrying behavior of a UHPC-stub column was presented during load application on the entire section. The ultimate forces and the mechanical behavior of the different specimens were compared in general the bearing capacity of columns was lower when the load was applied on the entire cross section than when the load was applied on the concrete exclusively.

Orgass and Klug (2004) [8] investigated the influence of short steel fibers and a fiber mix of short and long fibers on the mechanical properties of UHPC especially regarding the ductility and the size effect. In this regard the fiber contents changed between 0 and 1% volume fraction. Numerous tests were performed to study the flexural strength as well as the post cracking behavior of the investigated concrete. It was observed that highest compressive and flexural strengths were obtained on smallest specimens (prisms). In vibrated concrete the compressive strength was shown to decrease with the increase of the specimen slenderness. This phenomenon was not observed in self-compacting ultra-high performance concrete.

Washer *et al*. (2006) [9] reported on the development of ultrasonic methods for monitoring the elastic properties of UHPC under series of curing methods. Ultrasonic velocity measurements were used to estimate the bulk elastic modulus, shear modulus and Poisson's ratio of UHPC and results were compared with traditional destructive methods. Results indicated that the ultrasonic method was effective at tracking the development of modulus during air-curing of cylinders.

Ali (2007) [10] studied the performance of reactive powder concrete incorporating the High Reactivity Metakaolin (HRM) as pozzolanic admixture. The mixes were composed of ordinary portland cement, very fine sand (less than 600 μm), HRM which was mixed as an additive of 20 % by weight of cement, steel fibers, high range water reducing admixture at optimum dosage (10% by weight of cement). It was found that it is possible to produce RPC from HRM as a pozzolanic admixture, with compressive strength of 176 MPa at age of 28 days.

Redaelli and Muttoni (2007) [11] carried out tests on a series of large-scale unreinforced and reinforced UHPC beams, to investigate the effect of the amount and type of reinforcement on structural behavior. A simple analytical model was presented to describe the behavior of reinforced UHPC ties. The analytical equations of cracking and first yield were solved numerically to investigate the role of some physical parameters. The numerical study showed that the initial slope of the stress-crack opening relationship had an influence on the structural response at the first cracking stages.

Ibraheem (2008) [12] carried out an experimental investigation to establish the complete compressive stress - strain relationships for different RPC mixes. A general equation for expressing such relationships was derived. The mathematical properties of RPC including compressive strength, density, absorption, and flexural behavior were all established experimentally. In addition, an idealized compressive stress block for RPC sections under pure bending moment was proposed and used to derive an equation for calculating the nominal bending moment capacity (M_n) of singly reinforced rectangular RPC sections. The accuracy of the derived equation of M_n was examined by comparison with the experimental results.

Schachinger *et al*. (2008) [13] studied the effect of subjecting UHPC to a temperature of 90°C during its early ages (for 24 to 48 hours). It was shown that such heat treatment accelerated the pozzolanic reaction of silica fume with Ca $(OH)_2$ and resulted in high strength development of UHPC. The compressive strength of a heat treated UHPC was observed to increase from 220 to 280 MPa over 8 years' storage in water. The chain length of the C-S-H phases increased from values between 5 and 6 to 9 during this period. A distinct increase in compressive strength of UHPC not subjected to heat treatment was also observed at high ages. The compressive strength was 250MPa at an age of six years which was 58% more than the 28 day strength of 160MPa.

2. EXPERMENTAL WORK

Two different kinds of admixtures for ultra high performance concrete (namely, high reactivity metakaolin and silica fume) were used separately with three different steel fibers ratios (1.0 %, 1.5% or 2.0%) for each mix. Therefore the total number of UHPC mixes considered in this experimental investigation was six. From each specific UHPC mix, three cubes (50 mm×50 mm× 50 mm) are tested under uniaxial compression to assess the compressive strength of UHPC at 3,7, and 28 days of age.

2.1 Materials

2.1.1 Cement

Sulfate resisting portland cement is usually used in UHPC because it contains low C_3A content. Independent of other variables, mixes with cement of low C_3A content always require lower w/c ratios as compared to mixes with ordinary cement. Sulfate resisting portland cement manufactured in the Kingdom of Saudi Arabia named "Al-Sharqiya Cement" was used in this investigation. The chemical test of this type of cement was

VOL. 6, NO. 5, MAY 2011 ISSN 1819-6608
ARPN Journal of Engineering and Applied Sciences

www.arpnjournals.com

carried out by the National Center for Construction Laboratories and Research (NCCLR), and the results of the test indicate that the chemical compositions of the used cement conformed to the ASTM standard specification for Portland cement.

2.1.2 Fine aggregate

Al-Ekhaider natural sand of 4.75mm maximum size was used as fine aggregate. Results indicate that fine aggregate grading is within the requirements of the B.S. 882/1992 specification. For UHPC, very fine sand with maximum size 600μm was used. This sand was separated by sieving, its grading satisfied the fine grading in accordance with the B.S. specification No. 882/1992.

2.1.3 Steel fibers

Straight brass coated steel fibers 13 mm long with a diameter of 0.18 mm and an aspect ratio of 72 were used throughout the experimental program. A thin brass coating was applied to the fibers during the drawing process; therefore, virgin fibers were gold-colored. This coating disappeared during the mixing process and was no longer clearly visible during the casting of the UHPC.

2.1.4 Mixing water

Ordinary tap water was used for mixing and curing all the concrete specimens considered in this research.

2.1.5 Mineral admixtures

Mineral admixtures are finely ground solid materials that are used to replace part of the cement in a concrete mixture. These materials react chemically with hydrating cement to form a modified paste microstructure. These admixtures improve concrete workability, mechanical properties, and durability. Two types of mineral admixtures were used in this research: High Reactivity Metakaolin (HRM) and Silica Fume (SF).

2.1.5.1 High reactivity metakaolin (HRM)

Metakaolin is one of the most abundant natural minerals which produced by heat-treating kaolin,. Kaolin is a fine, white clay that has traditionally been used in the manufacture of porcelain. The term kaolin is derived from the name of metakaolin which typically contains 50-55% SiO_2 and 40-45% Al_2O_3. Other oxides are also present but in small amounts such as Fe_2O_3, TiO_2, CaO, and MgO. Metakaolin particles are generally one-half to five microns in diameter, an order of magnitude smaller than cement grains and larger than silica fume particles. Metakaolin is white in color.

2.1.5.2 Silica fume (SF)

A white undensified Silica Fume (SF) with Blaine fineness about 200(m^2/g) is a pozzolanic material which has a high content of amorphous silicon dioxide and consists of very fine spherical particles. It reacts with calcium hydroxide Ca $(OH)_2$, producing calcium silicate hydrate (secondary gel). It is added as partial replacement by weight of cement.

2.1.6 Chemical admixture

A high performance concrete superplasticizer (or named High Range Water Reduction Agent HRWRA) based on polycarboxylic technology, Structuro 335 in combination with Structuro 480, are high performance cohesion agent especially designed to ensure a good consistency and stability in concrete.

2.2 Concrete mixes

In order to study the influence of the different mixture ratios on the mechanical properties of Ultra High Performance Concrete, the following aspects have been considered;

a) Two types of mineral (pozzolanic) admixtures [namely: High Reactivity Metakaolin (HRM) and Silica Fume (SF)].
b) Three proportions of steel fibers (1.0%, 1.5%, 2.0%) for each type of mineral admixture.

This gives six different mixes which were used in this investigation as shown in Figure-1.

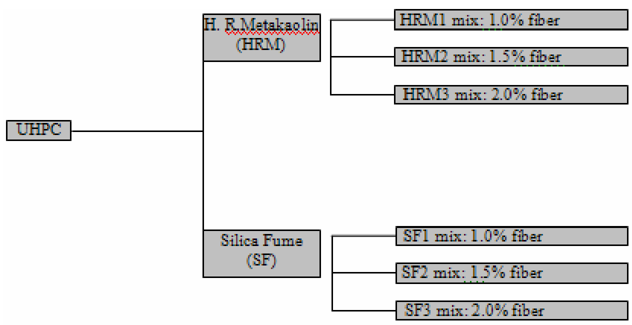

Figure-1. Mixes studied in the present investigation.

2.3 Compressive strength test

The compression tests were carried out on a standard 50 mm cubic specimens tested after curing at the ages of 3, 7, and 28 days for each mix. The average of three cubes was adopted for each age. The testing procedure was carried out using an Averey-Dension 2000kN capacity compression testing machine. Test results for compressive strength of various mixes of Ultra High Performance Concrete investigated in this study were summarized in Table-1. The Table shows the compressive strength values at three ages (3, 7 and 28 days). Results indicate that a 28 days compressive strength of 198MPa was obtained for SF3 mix (mix included Silica Fume and steel fibers of 2.0 % volume fraction) while a 28 days compressive strength of 159MPa was obtained for HRM3 mix (mix included High Reactivity Metakaolin and steel fibers 2.0 % volume fraction).

Table-1. Compressive strength of UHPC mixes at 3, 7, and 28 day's age (present study).

Mix	Cement (kg/m^3)	H. R. Metakaolin %	Silica fume %	Steel fibers %	w/c ratio	Compressive strength (MPa) 3 days	7 days	28 days
HRM1	850	15%	-----	1.0%	0.174	88	103	151
HRM2	850	15%	-----	1.5%	0.178	90	106	155
HRM3	850	15%	-----	2.0%	0.179	91	109	159
SF1	900	-----	10%	1.0%	0.186	98	122	191
SF2	900	-----	10%	1.5%	0.189	99	124	195
SF3	900	-----	10%	2.0%	0.19	102	127	198

Generally, all UHPC mixes showed initial rapid strength gain during early ages followed by a gradual decrease in the rate of strength gain. This can be attributed to the effect of water reduction on compressive strength, that is UHPC mixes because of their low water cementitious ratio gain strength more rapidly than mixes with higher water cement ratio, as the cement grains are closer together and a continuous system of gel is established more rapidly.

Also the results show that the addition of pozzolanic mineral admixtures (metakaolin or silica fume) can cause a considerable increase in compressive strength at early ages. That is mainly due to the fact that the chemical reaction of pozzolanic materials usually starts at early ages (3 and 7 days), and increases till the age of 28 days. This can be explained by the high pozzolanic reaction of particles of these materials with calcium hydroxide released from cement hydration leading to pore size and grain size refinement processes which can strengthen the microstructure and reduce the micro-cracking.

2.4 Compressive stress-strain relationships

The test setup included the specially designed axial deformation measuring device shown in Figure-2. The two parallel rings are both rigidly attached to the steel cylinder with a 10 mm gage length between attachment points. The upper ring holds a dial gage with sensitivity of 0.002 mm whose free end bears on the lower ring. This technique was used for the determination of both the ascending and descending portions of the stress-strain relationship. Two cylindrical concrete specimens for each mix were used in this study with dimensions of (75×150) mm. Also a high strength steel cylinder with dimensions of (150mm height, 100mm internal diameter, and 3mm thickness) was used in this study. The concrete specimen was placed inside the steel tube and care was taken to ensure that the top faces of both the concrete specimen and the steel tube were on the same horizontal level. A steel plate was put on the top of both the steel tube and the concrete specimen. In order to obtain a complete stress-strain relationship (the ascending and descending parts), it was essential to ensure that the high strength steel tube behaved elastically under the action of direct compression up to a value of strain equal to 0.006. The compressive stress-compressive strain relationships of all the UHPC specimens were obtained to a strain value of 0.006.

Figure-2. Device used to obtain stress-strain relationship.

In order to show the actual effect of each of the main variables in this research (which are the type of pozzolanic admixture and percentage of fibers) on the stress-strain curve of UHPC in compression, each variable will be studied separately by keeping the other two variables constant. The effect of each variable is shown in one Figure that contains set of curves designed to cover the whole range of the two variables.

A-Effect of varying the pozzolanic admixture

The effect of this variable on the experimental stress-strain curve of UHPC in compression is shown in Figure-3. It can be seen from this Figure that for any value of strain, the value of stress is highest for UHPC using Silica Fume (SF), and lowest for UHPC using High Reactivity Metakaolin (HRM). However the discrepancies in the values of such stresses are more pronounced in the descending parts than in the ascending parts of the stress-strain relationships. It can be concluded that a better strength of UHPC is achieved by using Silica Fume (SF) than Highr Reactivity Metakaolin (HRM).

VOL. 6, NO. 5, MAY 2011 ISSN 1819-6608
ARPN Journal of Engineering and Applied Sciences

www.arpnjournals.com

B-Effect of varying the percentage of fibers

Figure-3 shows the effect of varying the percentage of fibers on the compressive stress-strain curve of UHPC. The Figure shows only little variations during the ascending part but the effect is clear with higher discrepancies during the descending part of the stress-strain relationship. It can also be seen from this Figure that the change in the value of the percentage of fibers has little effect on the peak stress, which is higher for higher percentage of fibers.

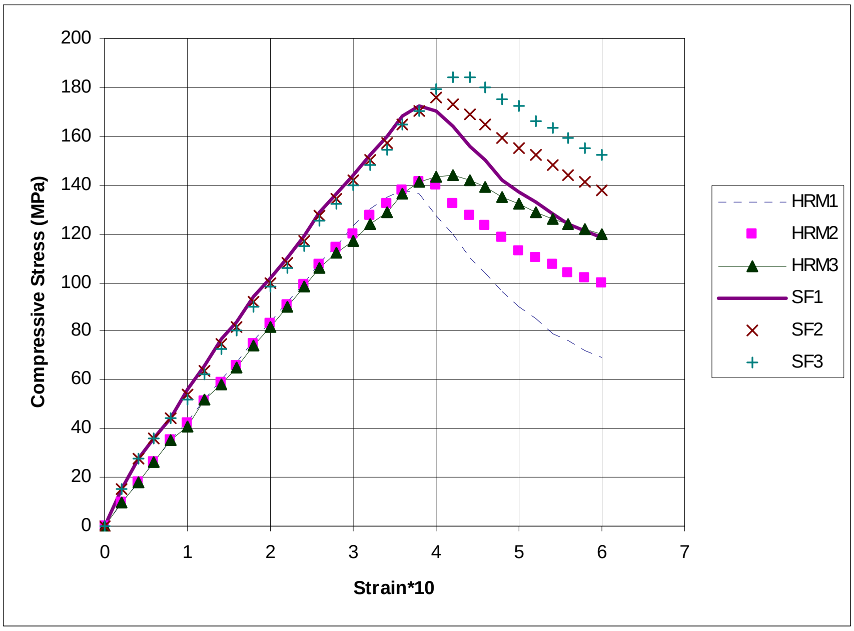

Figure-3. Stress-strain curve fro different ultra high performance concrete mixes.

3. FINITE ELEMENT ANALYSIS

The present study used the computer software ANSYS version 11(Analysis System) for performing the nonlinear model analysis. ANSYS is comprehensive general purpose finite element computer program that contains more than 180 different elements. This variety of elements allows the ANSYS program to analyze two- and three - dimensional structures, piping systems, two-dimensional plane and axisymmetric solids, flat plates, axisymmetric and three - dimensional shells and nonlinear problems including contact (interfaces) and cables. The program contains many special features which allow nonlinearities or secondary effects to be included in the solution, such as plasticity, large strain, hyper elasticity, creep, swelling, large deflections, contact, stress stiffening, temperature dependency and material anisotropy.

3.1 Concrete brick element

Concrete is represented by the SOLID65 isoparametric brick element shown in Figure-4. This element has successfully been used for three dimensional nonlinear RC analysis. This element has eight nodes with three degrees of freedom at each node (translations u, v, and w in the nodal x, y and z directions respectively). This element is capable of plastic deformation, cracking in three orthogonal directions and crushing.

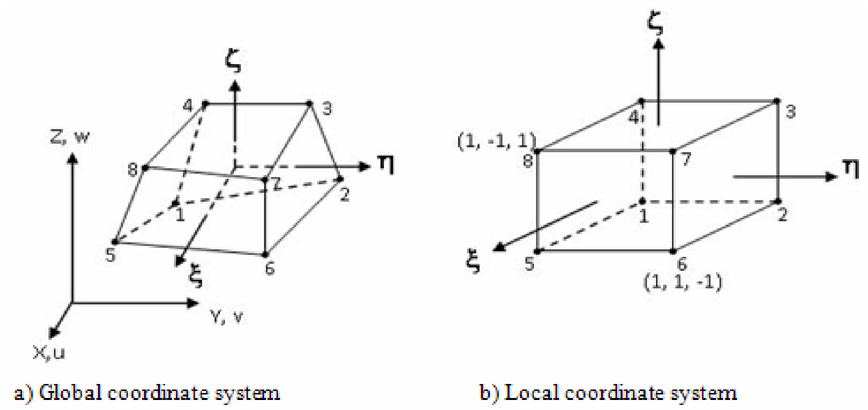

Figure-4. 8-node 3-D reinforced concrete solid element a) in global coordinates b) in local coordinates.

VOL. 6, NO. 5, MAY 2011 ISSN 1819-6608
ARPN Journal of Engineering and Applied Sciences

3.2 Reinforcement representation

Reinforcement is modeled using LINK8 bar (or truss) element which may be used in a variety of engineering applications. This 3-D spar element is a uniaxial tension-compression element with three degrees of freedom at each node. In translation in the nodal x, y, and z directions, as in a pin-jointed structure, no bending of the element is considered. This element is used in the present study to simulate the behavior of reinforcing bars which work as stirrups in resisting the vertical shear in concrete and main longitudinal steel reinforcement in resisting the flexural stresses. The geometry, node locations, and the coordinate system for the element are shown in Figure-5.

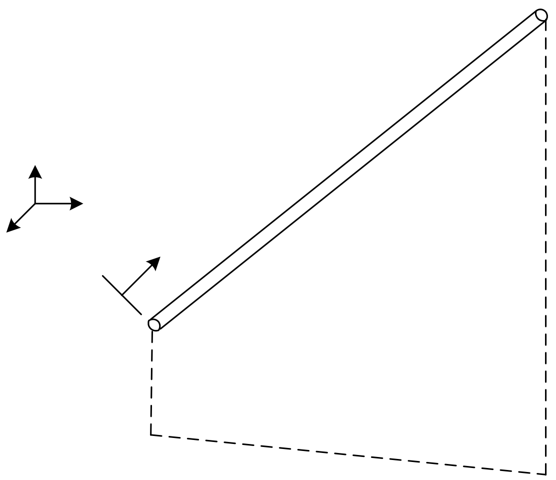

Figure-5. LINK8 - 3-D spar.

4. STRESS-STRAIN MODELS

Several approaches are available for defining the complicated stress-strain behavior of RC in compression under different states of stresses. The plasticity-based models have been introduced to account for the plastic flow ability of concrete before crushing. In these models, concrete can be modeled as a strain hardening material. The adopted plasticity based model is suitable for the nonlinear three-dimensional analysis of RC beams under monotonically increasing load.

4.1 Modeling of concrete in compression

The behavior of concrete in compression can be simulated in ANSYS-11 by an elasto-plastic work hardening model followed by a perfectly plastic response, which is terminated at the onset of crushing. The model used for compression is expressed in terms of yield criterion, a hardening rule and a flow rule. The yield criterion adopted in ANSYS-11 is the von-Misses criterion and the adopted hardening rule assumes that the yield surface expands uniformly without distortion as plastic deformation occurs.

In the present model, a multilinear stress-strain curve is used for the uniaxial stress-strain relationship beyond the limit of elasticity, $0.45f_c'$. This parabolic curve represents the work-hardening stage of behavior. When the peak compressive stress is reached, a perfectly plastic response is assumed to occur. Figure-6 shows the equivalent uniaxial stress-strain curve adopted by ANSYS-11 at various stages of loading. To construct the stress-strain relationship in the plastic range, an associated flow rule is usually employed. This means that the plastic deformation rate vector will be assumed normal to the yield surface.

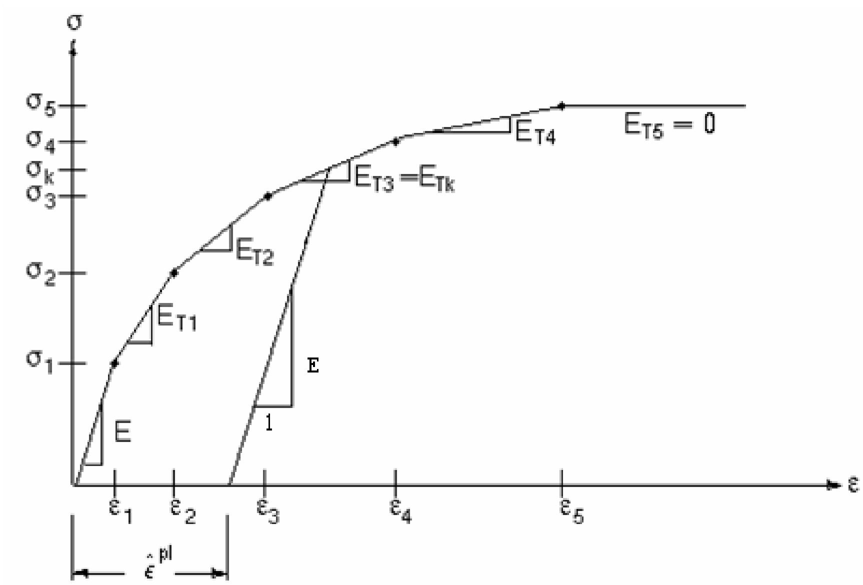

Figure-6. Multilinear stress-strain curve for concrete adopted in the analysis.

VOL. 6, NO. 5, MAY 2011 ISSN 1819-6608
ARPN Journal of Engineering and Applied Sciences

www.arpnjournals.com

4.2 Behavior of concrete in tension

In the ANSYS-11, the onset of cracking is controlled by a maximum principal stress criterion. A smeared crack model with fixed orthogonal cracks and the tension stiffening concept (to describe the post cracking response of concrete) are adopted in the present study. Since, the cracked concrete can still initially carry some tensile stresses in the direction normal to the crack, the tension-stiffening effect is considered. This has been achieved in ANSYS-11 by assuming gradual release of the concrete stress component normal to the cracked plane. In the present work, the normal stress that is carried by cracked concrete can be obtained from Figure-7. The shear transfer coefficient for an open crack is β_0 and the shear transfer coefficient for a closed crack is β_1.

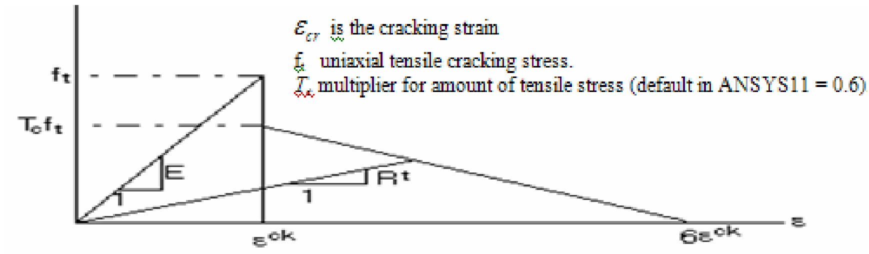

Figure-7. Post cracking model for concrete used in the present analysis.

4.3 Crushing modeling

If the material at an integration point fails in uniaxial, biaxial or triaxial compression, the material is assumed to crush at that point. Under this condition, the material strength at the considered integration point is assumed to have degraded to an extent such that its contribution to the stiffness of an element in question can be ignored (ANSYS-11).

5. APPLICATIONS

The applications are made in order to verify the ability of the adopted nonlinear finite element model to investigate the flexural behavior of UHPC beams. The accuracy and validity of the computer program to predict the load carrying capacity of the analyzed beams are also investigated. Two examples are considered, each example deals with a particular aspect of behavior. These examples are:

Simply supported unreinforced UHPC deep beam (B1) tested by Collepardi *et al*. (1996) [2].

Simply supported reinforced UHPC thin beam (B2) tested by Ibraheem (2008) [12].

5.2 Unreinforced concrete deep beam (B1)

Collepardi *et al*. (1996) [2] carried out a series of flexural tests of unreinforced UHPC beams to create an understanding of load-deflection behavior of such beams with different mixes. The selected beam was a control beam designated as (B1). Beam (B1) was simply supported over a 450mm span and had 150mm width with 150mm depth. The beam was unreinforced and was subjected to two-point loads. By making use of symmetry of loading and geometry, only one-half of the beam has been considered for the finite element analysis. The chosen segment was modeled using 6975 (8-node) brick elements. The concentrated loads were modeled as line loads uniformly distributed across the width of top surface. The total applied load was 150 kN. The finite element analysis was carried out using 8-points integration rule, with a convergence tolerance of 5%. The shear transfer coefficients for an open crack β_0=0.2 and the shear transfer coefficients for a closed crack β_1=0.8. The finite element mesh, boundary and symmetry conditions and loading arrangement used are shown in Figure-8. Material properties and additional material parameters adopted in the analysis are shown in Table-2.

ARPN Journal of Engineering and Applied Sciences

www.arpnjournals.com

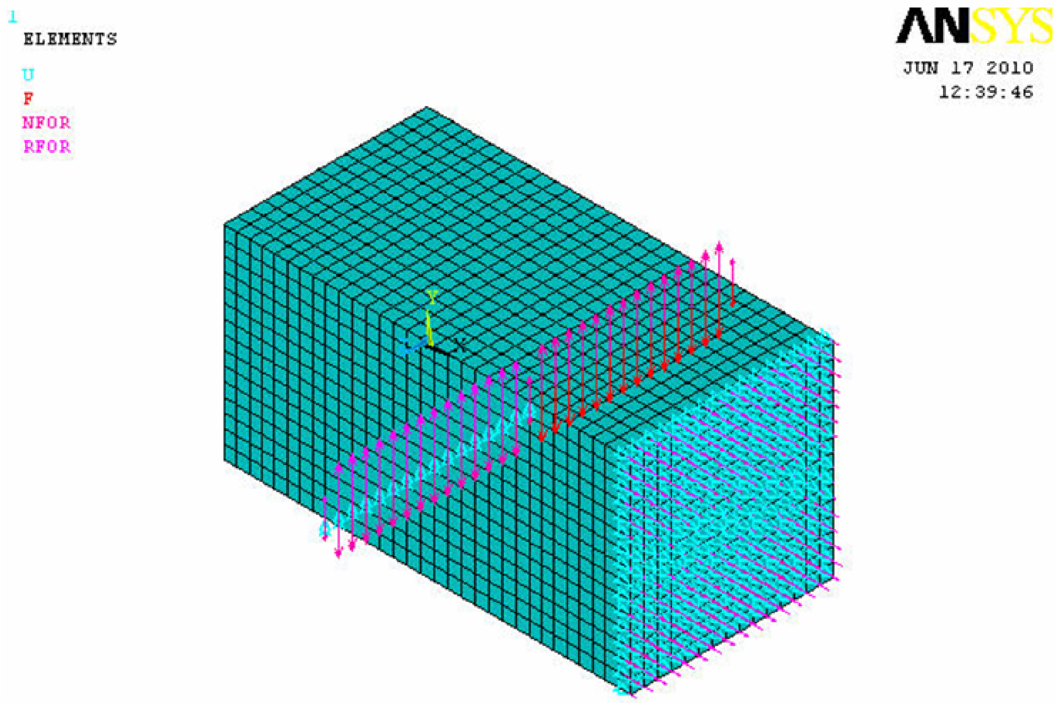

Figure-8. Finite element mesh, loading and boundary conditions used for UHPC deep beam (B1).

Table-2. Material properties and material parameters used for UHPC deep beam (B1) [2].

Concrete		
E_c	Young's modulus (MPa)*	57143
f_c`	Compressive strength (MPa)	150
f_t	Tensile strength (MPa) **	6
v_c	Poisson's ratio**	0.2
Stress-strain relationship for concrete in compression		
	Strain	**Stress** (MPa)
Point 1	0.00105	60
Point 2	0.00164	83.62
Point 3	0.00223	103.4
Point 4	0.002826	120.41
Point 5	0.00341	135.85
Point 6	0.0040	150
Point 7	0.005	150

* $E_c = 4700\sqrt{f_c'}$, ** Assumed values in ANSYS

The experimental and numerical load-deflection curves obtained for UHPC beam (B1) are shown in Figure-9. The finite element solution is in acceptable agreement with the experimental results throughout the entire range of loading. A relatively softer numerical response is noticed at stages close to the ultimate load. The numerical ultimate load was slightly lower than the experimental value. The numerical ultimate load was (130kN), while the experimental ultimate load was (134kN). The ratio of the predicted ultimate load to the experimental value is (0.97). Variation in deflection along the selected half of beam (B1) at ultimate load is illustrated in Figure-10. Distribution of concrete normal stress in the longitudinal x-direction (SX), along the selected half of beam (B1) at the ultimate load is shown in Figure-11. In this Figure, it is obvious that the higher compressive stresses are located at mid-span where the upper fibers of the cross section being in compression and the lower fibers in tension. The maximum recorded compressive stress (-108.86MPa) is located directly under the applied load.

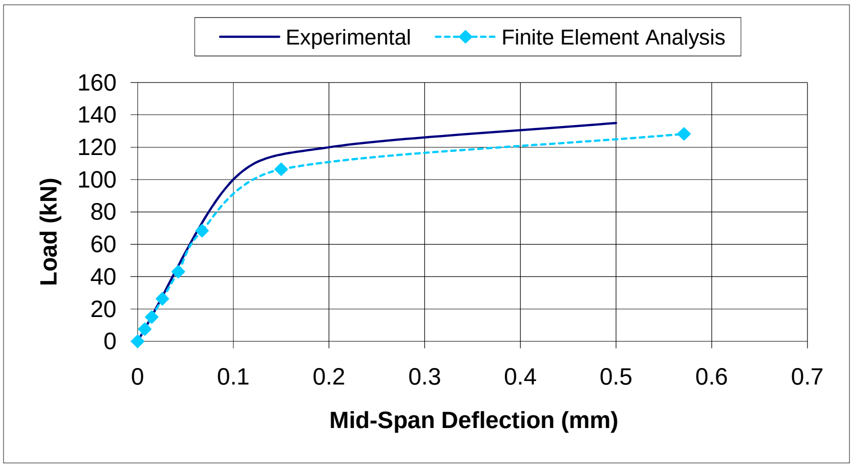

Figure-9. Experimental and numerical load-deflection behavior of UHPC beams (B1).

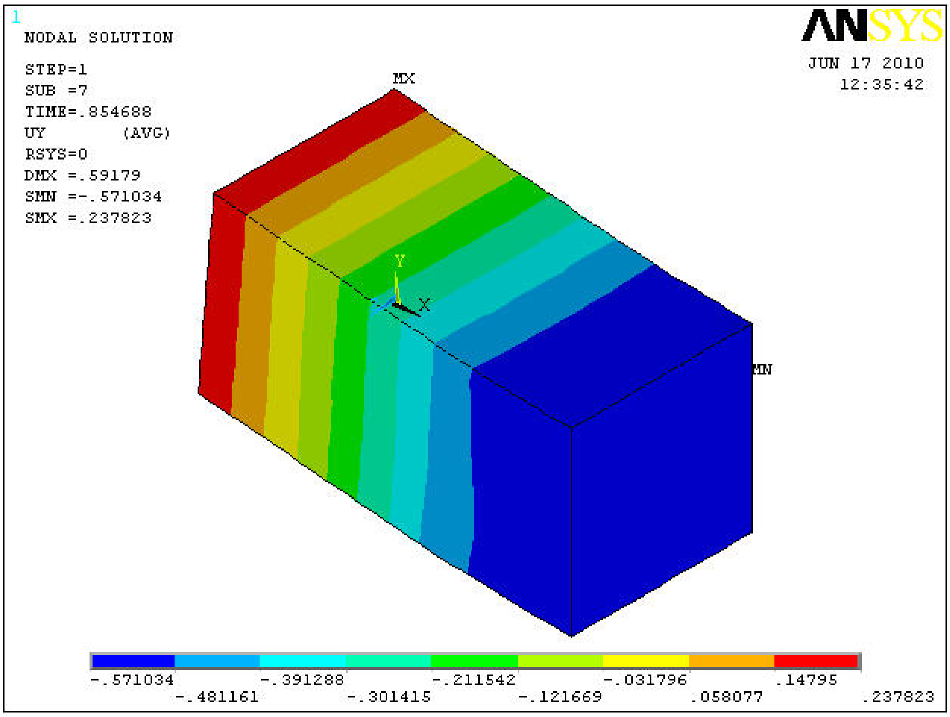

Figure-10. Variation in deflection UY along the selected quarter of UHPC beam (B1) at ultimate load.

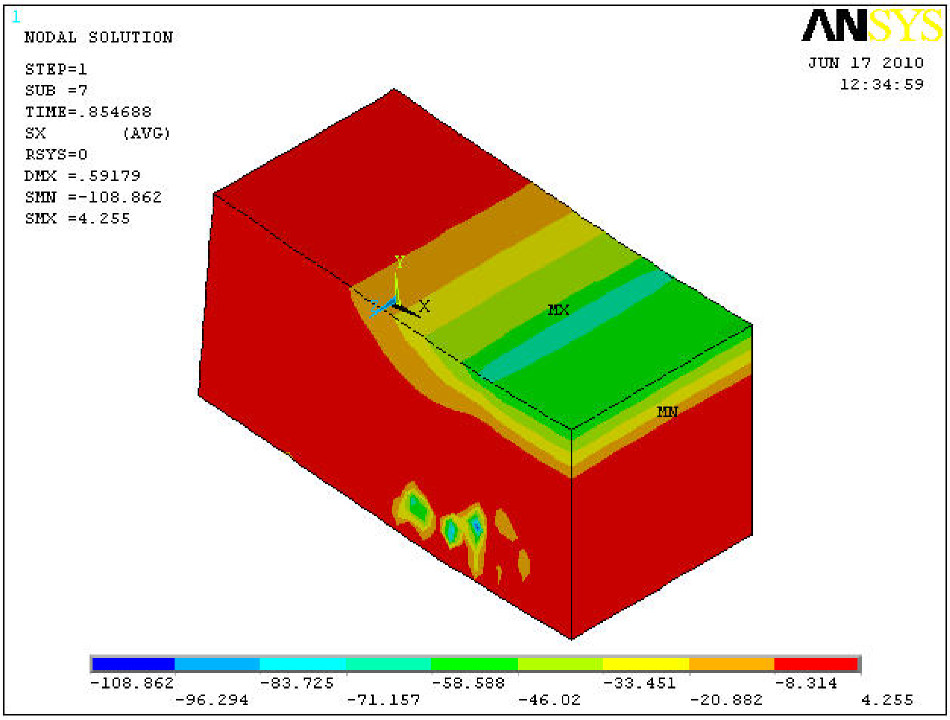

Figure-11. Variation in normal stress (σ_x) along the selected quarter of UHPC beam (B1) at ultimate load.

5.3 Reinforced concrete thin beam (B2)

Ibraheem (2008) [12] carried out a series of tests to create an understanding of flexural failure of reinforced UHPC beams. The selected beam was a control beam designated as (B2). Beam (B2) was simply supported over a 600mm span and had 200mm width with 50mm depth. The beam was reinforced with longitudinal deformed steel bars and stirrups. The concrete mix contains 15% metakaolin and 1.25% steel fibers. The beam was subjected to two-point loads. The total applied load was 10 kN. The loading arrangement and reinforcement details together with the overall geometry of the beam are shown in Figure-12.]

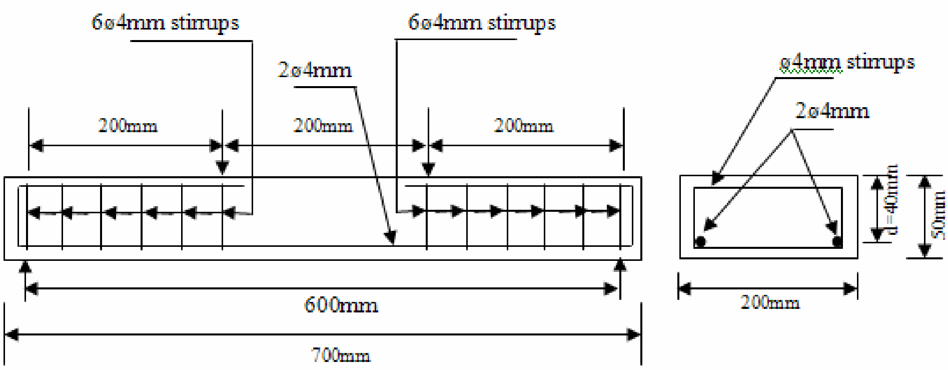

Figure-12. Dimensions and loading arrangement of UHPC thin beam (B2) [12].

By making use of symmetry of loading, geometry and reinforcement distribution, only one-half of the beam has been considered for the finite element analysis. The chosen segment was modeled using 3500 (8-node) brick elements and 318 link 8 elements. The main and shear reinforcement were modeled using discrete representation. The concentrated loads were modeled as line loads uniformly distributed across the width of top surface. The finite element analysis was carried out using 8-point integration rule, with a convergence tolerance of 5%. The shear transfer coefficients for an open crack β_0=0.2 and the shear transfer coefficients for a closed crack β_1=0.8. The finite element mesh, boundary and symmetry conditions and loading arrangement used are shown in Figures 13 and 14. Material properties and additional material parameters adopted in the analysis are shown in Table-3.

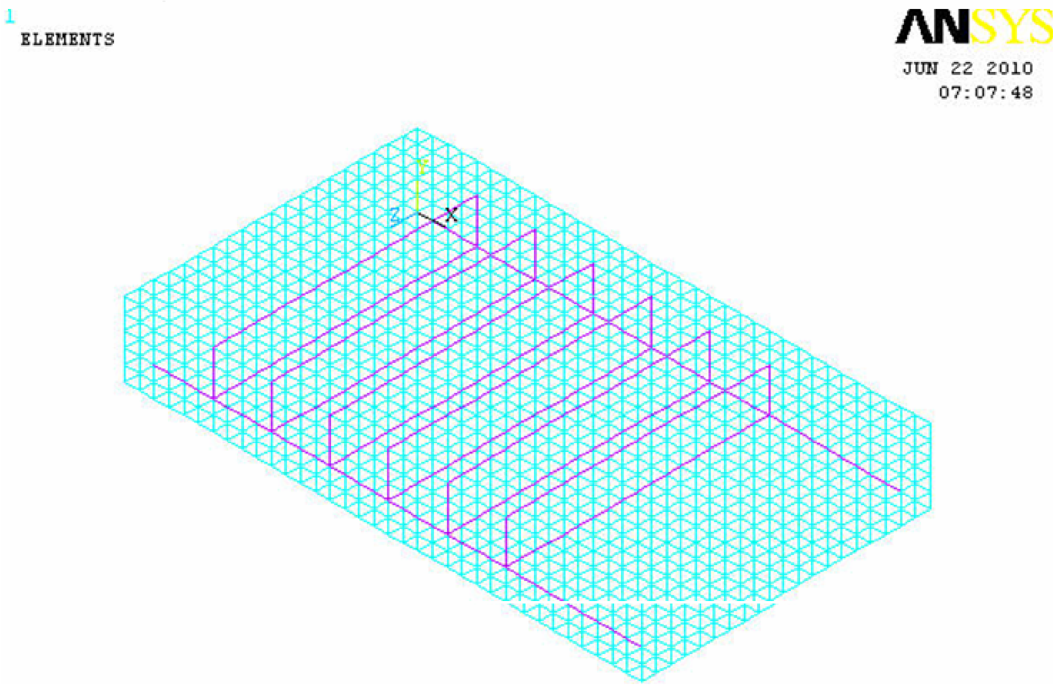

Figure-13. Finite element mesh used for UHPC thin beam (B2).

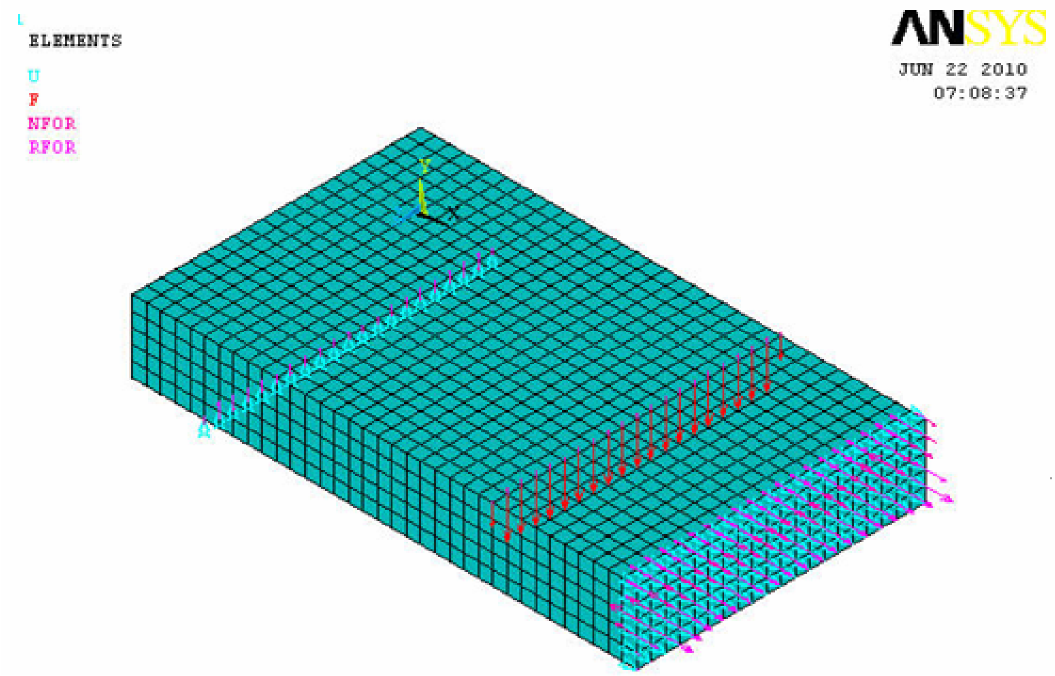

Figure-14. Boundary and symmetry conditions used for UHPC thin beam (B2).

ARPN Journal of Engineering and Applied Sciences

Table-3. Material properties and material parameters used for UHPC thin beam (B2) [12].

Concrete		
E_c	Young's modulus (MPa)	40500
f_c`	Compressive strength (MPa)	144
f_t	Tensile strength (MPa)*	3.5
v_c	Poisson's ratio*	0.2
Longitudinal and stirrups reinforcement		
E_s	Young's modulus (MPa)*	200000
f_y	Yield stress (MPa)	400
v_s	Poisson's ratio*	0.3
A_s	Area of single longitudinal bars (mm^2)	12.6
Stress-strain relationship for concrete in compression		
	Strain	**Stress** (MPa)
Point 1	0.0016	64.8
Point 2	0.00212	84.10
Point 3	0.00264	101.13
Point 4	0.00316	116.56
Point 5	0.00368	130.77
Point 6	0.0042	144
Point7	0.005	144

* Assumed values in ANSYS

The experimental and numerical load-deflection curves obtained for UHPC beam (B2) are shown in Figure-15. The finite element solution is not in acceptable agreement with the experimental results for the most range of loading. A relatively stiffer numerical response is noticed with increasing load. The experimental results show higher displacement at lower stage of loading which is different from the exact deflection for linear elastic concrete modeling (about 14 times). The used computer program is restricted to the used models and there is no way to add new subroutine to get a better simulation of the UHPC thin beams behavior. The numerical ultimate load was slightly higher than the experimental value. The numerical ultimate load was (7.09kN), while the experimental ultimate load was (7kN). The ratio of the predicted ultimate load to the experimental value is (1.013). Variation in deflection along the selected quarter of beam (B2) at ultimate load is illustrated in Figure-16. Distribution of cracks in concrete along the selected quarter of beam (B2) at the ultimate load is shown in Figure-17.

ARPN Journal of Engineering and Applied Sciences

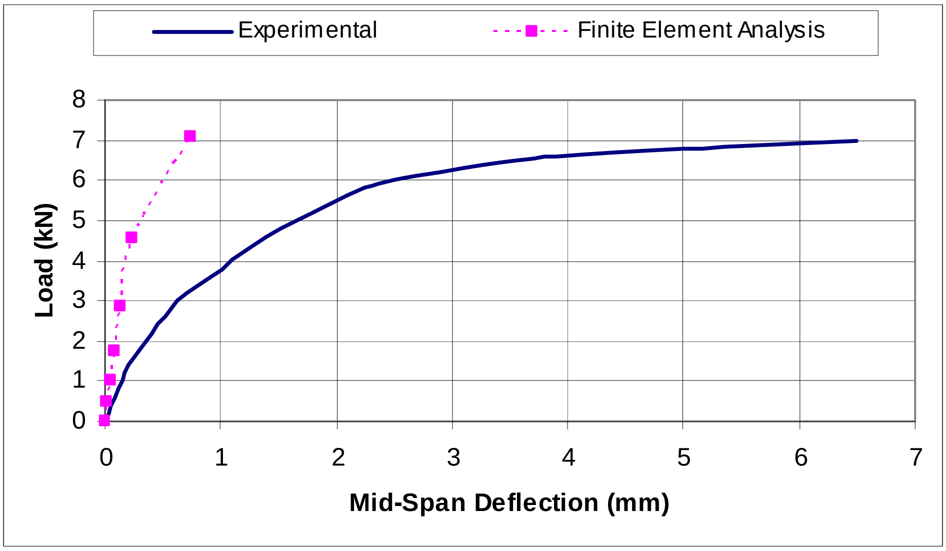

Figure-15. Experimental and numerical load-deflection behavior of UHPC beams (B2).

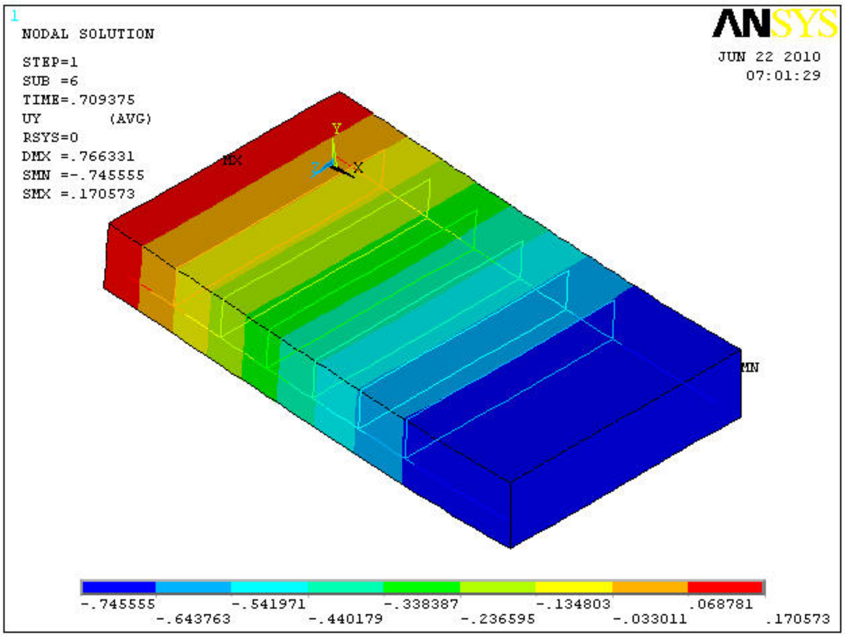

Figure-16. Variation in deflection UY along the selected quarter of UHP beam (B2) at ultimate load.

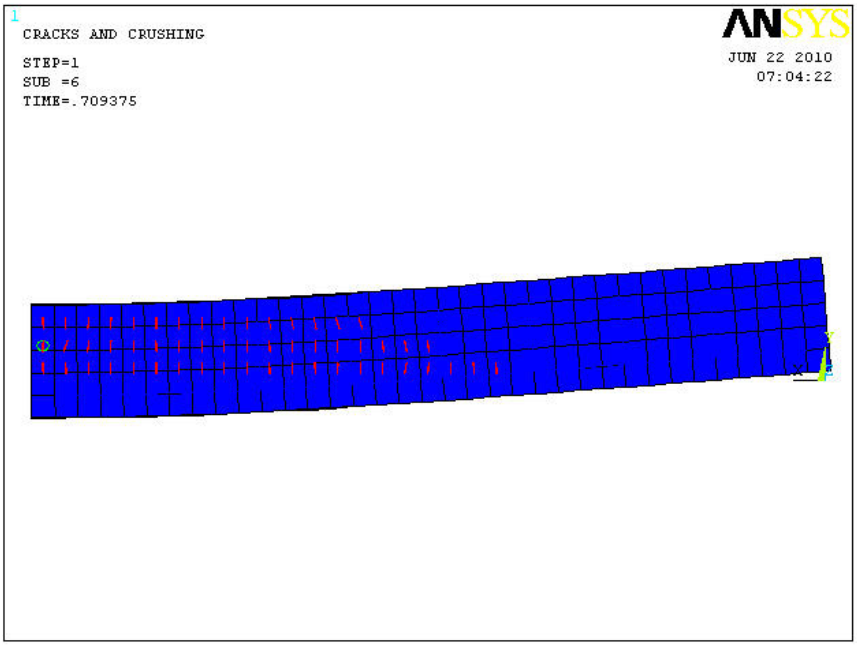

Figure-17. Crack pattern along the selected quarter of UHPC beam (B2) at ultimate load.

6. CONCLUSIONS

Depending on the results of the tests carried out on different UHPC mixes, and based on the analysis, discussions, and comparisons with corresponding theoretical predictions, the following conclusions can be drawn:

a) For all UHPC mixes, a great percentage of compressive strength was obtained at early ages of concrete, and that was because of the steam treatment adopted in this study. Results exhibit high compressive strengths for all UHPC mixes but with some differences in values due to the variables adopted in these UHPC mixes. In general, UHPC mixes with silica fume (SF) showed the highest value of cube compressive strength at different ages and for different steel fibers volume fraction;
b) Increasing the steel fibers volume fraction will increase the cube compressive strength for different pozzolanic admixture. The results show that the cube compressive strength of UHPC will be increased by not more than 5% when the percentage of fibers in the mix is increased from 1.0 % to 2.0%;
c) In general, the results obtained using the finite element models represented by the load midspan deflection curves show good agreement with the experimental data of deep beam (B1) considered in this study. The difference between the numerical ultimate loads and the corresponding experimental ultimate loads for deep beam (B1) and thin beam (B2) are 3% and 4% respectively;
d) The experimental results for the compressive stress-compressive strain relationships of different UHPC mixes, showed that for any value of strain, the value of stress is highest for UHPC mixes using (SF), and lowest for UHPC mixes using (HRM); and
e) The amount of fibers in an UHPC mix was found to have little effect on the ascending part of the compressive stress - compressive strain relationship but clear differences were obtained for the descending part of the relationship.

REFERENCES

[1] A. R. Lubbers. 2003. Bond Performance between Ultra-High Performance Concrete and Prestressing Strands. Faculty of Fritz, College of Engineering and Technology of Ohio University. pp. 155-165.

[2] S. Collepardi, L. Coppola, R. Troli and M. Collepardi. 1996. Mechanical Properties of Modified Reactive Powder Concrete. International Conference on Super plasticizers and the Chemical Admixtures in Concrete, Rome, Italy, Farmingto Hills, ACI Publication SP-173. pp. 1-21.

[3] B.A. Graybeal and P.E. Hartmann. 2000. Ultra-High Performance Concrete Material Properties. Transportation Research Board Conference. pp. 1-14.

[4] N. Roux, C. Andrade and M. A. Sanjuan. 1996. Experimental Study of Durability of Reactive powder Concretes. ASCE Journal of Materials in Civil Engineering. 8(1): 6-25.

[5] X. Qian and Z. Li. 2001. The Relationships between Stress and Strain for High-Performance Concrete with Metakaolin. Cement and Concrete Research Journal. 31: 1607-1611.

[6] P. Stähli and J. G. M. Mier. 2004. Three Fiber Type Hybrid Fiber Concrete. In proceeding FRAMCOS-5, Vail, USA. pp. 1105-1112.

[7] H. Schneider, G. Smisch and D. Schmidt. 2004. Bearing Capacity of Stub Columns Made of NSC, HSC, and UHPC Confined by a Steel Tube. Cement and Concrete Research, Dipl. - Ing., Institute for Massivbau, University of Leipzig, Lacer No. 9. pp. 122-130.

[8] M. Orgass and Y. Klug. 2004. Steel Fiber Reinforced Ultra-High Strength Concrete. Dipl.-Ing., Institute for Structural Concrete and Building Materials, University of Leipzig, MFPA Leipzig GmbH, Lacer No. 9. pp. 12-20.

[9] G. Washer, P. Fuchs, A. Rezai and H. Ghasemi. 2006. Ultrasonic Testing for Quality Control of Ultra-High Performance Concrete. Turner-Fairbank Highway Research Center, Mclean, VA 22101, ASCE, Structures. pp. 88-120.

[10] A. S. Ali. 2007. Mechanical Properties and Durability of Polymer Modified RPC Exposed to Oil Products. Ph.D. Thesis, University of Technology, Baghdad, Iraq. p. 180.

[11] D. Redaelli and A. Muttoni. 2007. Tensile Behavior of Reinforced Ultra-High Performance Fiber Reinforced Concrete Elements. Symposium Dubrovnik, Concrete Structures - Stimulators of Development. pp. 267-274.

[12] S. Kh. Ibraheem. 2008. Stress-Strain Relationships of Reactive Powder Concrete. Ph.D. Thesis, University of Technology, Baghdad, Iraq. p. 166.

[13] I. Schachinger, H. Hilbig and T. Stengel. 2008. Effect of Curing Temperature at an Early Age on Long-Term Strength Development of UHPC. 2nd International Symposium on Ultra High Performance Concrete, Kassel, 05-07 March. pp. 205-212.